An Indirect Laser-Induced Temperature Jump Determination of the Surface pK_a of 11-Mercaptoundecanoic Acid Monolayers Self-Assembled on Gold

John F. Smalley,* Keli Chalfant, and Stephen W. Feldberg

Department of Applied Science, Brookhaven National Laboratory, Upton, New York 11973-5000

Tal M. Nahir[†] and Edmond F. Bowden

Department of Chemistry, North Carolina State University, Raleigh, North Carolina 27695-8204

Received: August 7, 1998; In Final Form: January 13, 1999

The indirect laser-induced temperature jump (ILIT) method is used to determine the acidity (pK_a) of monolayers composed of 11-mercaptoundecanoic acid (MUA) self-assembled on vapor-deposited gold film electrodes in contact with either 0.10 or 1.0 M ionic strength $NaClO_4$ electrolyte solutions. The ILIT technique may be used to measure the pK_a of a surface-attached acid because the magnitude of the ILIT response is related to the potential gradient at the electrode/electrolyte interface which is, in turn, related to the extent of ionization of the acid. The relevant data are the potentials of zero ILIT response versus pH. A simple two-layer model of the acid-modified electrode/electrolyte interface and Gouy−Chapman double layer theory (modified for the onset of dielectric saturation effected by the large concentration of charge present at this interface when a substantial fraction of the carboxylic acid moieties are ionized) were employed to analyze these data. This analysis gives pK_a = 5.7 ± 0.2 at 0.10 M ionic strength and pK_a = 4.4 ± 0.2 at 1.0 M ionic strength while the total concentration of MUA comprising the self-assembled monolayer is determined to be essentially the same at both ionic strengths, averaging (5.4 ± 0.3) × 10^{-10} mol/cm^2. Reasons for the observed variation of pK_a with ionic strength are discussed.

Introduction

There is a continuing interest in chemisorbed films composed of organosulfur compounds self-assembled on various metals. These self-assembled monolayers (SAMs) produce well-ordered organic surfaces and interfaces which have a wide variety of scientific and technological applications.[1,2] SAMs containing acidic (or basic) groups are of particular interest because these monolayers are good model systems for the study of proton transfer reactions which are, in turn, relevant to many fields such as surface wetting,[3] emulsion stability,[3] and the biophysical stability of membranes.[4] SAMs containing ionized terminal carboxylic acids may also be used as well ordered substrates for the crystallization of inorganic salts[5] or the attachment of redox active compounds (e.g., cytochrome *c*[6−8]) to electrode surfaces at well-defined distances.

Several techniques have been used to determine the acidity (pK_a) of monolayers composed of thiols terminated by acid groups self-assembled on gold. These techniques include contact angle titration,[3,9,10] piezoelectric quartz crystal microbalance,[11] and voltammetric measurements on gold[12a] and silver[12b] electrodes coated with these SAMs. (The analysis of the data obtained from this last technique can be based upon the theory of the interfacial potential distribution of electrodes coated with molecular films which has been proposed by Smith and White.[13,14]) Surface-enhanced Raman spectroscopy has also been used to study monolayers composed of either 4-pyridinethiol, methyl red (coupled to cystamine), or cresol red (also coupled to cystamine) self-assembled on silver.[15]

In the present study, the indirect laser-induced temperature jump (ILIT) technique is used to determine the pK_a of monolayers composed of 11-mercaptoundecanoic acid (HS-$(CH_2)_{10}$COOH) self-assembled on vapor-deposited gold film electrodes. The pK_a of a surface-attached acid is defined as the value of the pH of the solution in contact with the monolayer when half of the acid functional groups are ionized.[10] In the ILIT technique, a rapid (<10 ns) change in the open-circuit potential of an electrode/electrolyte interface is effected by a small (2−5 °C) laser-induced temperature perturbation of this interface. This technique may be used to determine the pK_a's (or pK_b's) of self-assembled monolayers containing acidic (or basic) groups because the magnitude of the ILIT response is related to the potential gradient at the electrode/electrolyte interface which is, in turn, related to the extent of ionization of the surface-attached acid (or base). The use of an interfacial potential to measure the pK's of acids (or bases) adsorbed at an interface has been demonstrated by Eisenthal and coworkers[16,17] who have shown that this potential is a function of the second harmonic (SH) signal generation from the interface (i.e., the SH signal generation from the interface may be used to measure the interfacial electric field which is, in turn, related to the extent of ionization of the adsorbed acid (or base)). The SH signal from an aqueous/solid or air interface is the result of a combination of the second-order nonlinear polarizability ($\chi^{(2)}$, which is independent of the interfacial electric field) of the interface and a third-order process (in which the electric field generated by the presence of a surface charge can orient and induce a third-order polarization in the aqueous solvent).[16−18] However, the direct illumination of an interface with the large pulsed laser intensities needed to obtain measurable SH signals

[†] Present address: Department of Chemistry, California State University, Chico, CA 95929-0210.

10.1021/jp983325z CCC: $18.00
Published on Web 03/11/1999

may cause complicating (for SH data analysis) photochemical and direct thermal effects to the interface.[19]

In the present case, the electrode/electrolyte interface is assumed to be adequately described by the simple two layer model of Smith and White.[14] In this model, all acidic moieties are assumed to lie in the same plane (the plane of acid dissociation or PAD) at the terminus of the SAM, and the diffuse double layer starts at the PAD and extends into the electrolyte solution. The first layer includes the entire SAM up to the ionizable functional group, and the second layer is the diffuse double layer. The (open-circuit) potential (E) between the gold electrode and a reference electrode then is given by

$$E = \frac{\sigma_M}{C_T} + \frac{\sigma_{A/B}}{C_{dl}} + V_D \quad (1)$$

where the capacitance C_T is a series combination of the (integral) capacitance associated with the monolayer up to the PAD (C_{film}, F/cm^2) and the (integral) capacitance associated with the diffuse double layer (C_{dl}, F/cm^2), σ_M is the concentration of charge on the gold electrode, $\sigma_{A/B}$ is the concentration of charge associated with the fraction of the acid moieties which are ionized, and V_D is the dipole potential associated with this system which includes dipoles within the monolayer. For a small temperature change (ΔT), it is straightforward to deduce that

$$\Delta E/\Delta T = -(E - V_D)\frac{d \ln [C_T]}{dT} - \frac{\sigma_{A/B}}{C_{dl}}\left(\frac{d \ln [C_{dl}]}{dT} - \frac{d \ln [C_T]}{dT} - \frac{d \ln K_D}{dT}\left(\frac{[H^+]}{[H^+] + K_D}\right)\right) + \frac{dV_D}{dT} \quad (2)$$

where the quantity dV_D/dT includes the Soret potential induced by the difference in temperature between the electrode and the bulk (electrolyte) solution[20] and K_D is the dissociation constant of the surface-attached acid. Based on eq 1, K_D is given by[14,15]

$$K_D = K_\infty \exp\left[\frac{F}{RT}\left[\frac{\sigma_{A/B}}{C_{dl}}\left(1 - \frac{C_T}{C_{dl}}\right) + \frac{C_T}{C_{dl}}(E - V_D)\right]\right] \quad (3a)$$

where K_∞ is the dissociation constant of the acid at infinite ionic strength (where C_{dl} is also infinite[21]). Because C_T/C_{dl} is always $\ll$1.0 for the monolayers and ionic strengths investigated in the present study, eq 3a may be simplified to

$$K_D = K_\infty \exp\left[\frac{F\sigma_{A/B}}{RTC_{dl}}\right] \quad (3b)$$

This simplification of eq 3a removes the explicit dependence upon potential (E and, therefore, upon σ_M) from K_D so that

$$pH = pK_\infty - \log\left[-\left(\frac{\Gamma_T F}{\sigma_{A/B}} + 1\right)\right] - \frac{F\sigma_{A/B}}{2.3RTC_{dl}} \quad (4)$$

where Γ_T (mol/cm^2) is the total concentration of (both ionized and neutral) carboxylic acid moieties and $\sigma_{A/B}$ is negative.

Because the temperature change in the ILIT technique is so rapid, it is difficult to measure ΔT in eq 2. We have developed a technique for measuring the ΔT based upon the measurement (using a piezoelectric transducer) of the pressure pulse induced by the rapid interfacial temperature jump.[22] We believe that this technique gives an accurate measurement of ΔT. However, it would be better if the ILIT data used to determine the pK_a were independent of this determination of ΔT. This is accomplished by determining the potential (E_{pzr}) at which the ILIT response ($\Delta E/\Delta T$ in eq 2) is zero. From eqs 2 and 3b, E_{pzr} is given by

$$E_{pzr} = V_D + \frac{dV_D/dT}{d \ln [C_T]/dT} - \frac{\sigma_{A/B}}{C_{dl}}\left[\frac{d \ln [C_{dl}]/dT}{d \ln [C_T]/dT} - 1 - \frac{d \ln K_D/dT}{d \ln [C_T]/dT}\left(\frac{[H^+]}{[H^+] + K_D}\right)\right] \quad (5)$$

where

$$\frac{d \ln K_D}{dT} = \frac{\frac{d \ln K_\infty}{dT} - \left(\frac{F\sigma_{A/B}}{RTC_{dl}}\right)\left(\frac{1}{T} + \frac{d \ln [C_{dl}]}{dT}\right)}{\left[1 - \left(\frac{F\sigma_{A/B}}{RTC_{dl}}\right)\left(\frac{[H^+]}{[H^+] + K_D}\right)\right]} \quad (6)$$

Thus, because $\sigma_{A/B}$ is a function of pH, E_{pzr} will vary with pH. If $\sigma_{A/B}$ (and, consequently, K_D, see eqs 3a and 3b above), d ln K_∞/dT, d ln $[C_T]/dT$, d ln $[C_{dl}]/dT$, C_{dl}, V_D, and dV_D/dT, are all independent of potential, a plot of $\Delta E/\Delta T$ versus E (eq 2) will be linear so that E_{pzr} may be obtained from such a plot (as its intercept with the potential axis) even when E_{pzr} is not in an accessible range of potential.

The potentials of zero (ILIT) response were determined for SAMs composed of $HS(CH_2)_{10}COOH$ as a function of pH at 0.10 and 1.0 M ionic strength. At a particular ionic strength, the E_{pzr}'s were then fitted to a combination of eqs 4, 5, and 6 resulting in values of V_D, dV_D/dT, Γ_T, K_∞, d ln K_∞/dT, and pK_a at each ionic strength. For these fits, C_{dl} and d ln $[C_{dl}]/dT$ were calculated using Gouy−Chapman theory[3,13,17,21] modified for the onset of dielectric saturation[23] caused by the large concentration of charge ($\sigma_{A/B}$) which exists at the SAM/electrolyte solution interface when a significant fraction of the carboxylic acid moieties are ionized.

Experimental Section

Equipment, Materials and Methods. The ILIT apparatus, cell and experimental techniques have all been described in detail elsewhere.[19,22,24] A single modification was made to the ILIT cell for the present study. That is, the psuedo-reference electrode (see Figure 2 in ref 22 and Figure 3 in ref 24) has been moved closer to the working electrode. The psuedo-reference electrode now forms a truncated cone "above" the working electrode with the base of the cone being only ~3 mm away from the surface of the working electrode. This modification enables us to perform ILIT experiments at lower electrolyte concentrations (ionic strengths) than with the previous design of the ILIT cell.

As before,[22,24] the gold film electrodes used in this work were vapor deposited over a titanium underlayer (~500 Å thick) on quartz substrates (1 in. diameter disks, made of Homosil quartz by Heraeus Amersil). The total (gold plus titanium) thickness of these electrodes was ~1.0 μm. The titanium underlayer causes a uniform orientation of the 111 facets of the gold microcrystallites comprising the vapor-deposited gold layer.[25] The area of these electrodes was 0.71 cm^2, and they were cleaned in an argon ion plasma before use.[24]

The synthesis of the 11-mercaptoundecanoic acid (MUA) is also described elsewhere.[26] A clean electrode was placed in an ethanol solution containing 1.0×10^{-3} M of the MUA for approximately 3 days. (Note that we do not use any alkanethiol diluent in these experiments.[3,22]) The electrode is then taken

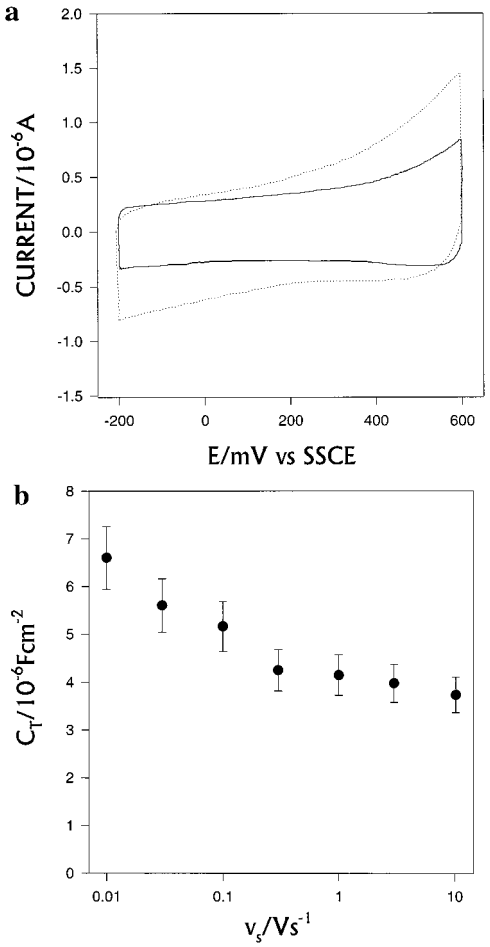

Figure 1. (a) Cyclic voltammograms of Au electrodes coated with monolayers of 11-mercaptoundecanoic acid. Solid line curve: ionic strength = 0.10 M, pH = 2.16, and T = 22.0 °C. Dotted line curve: ionic strength = 1.0 M, pH = 2.07, and T = 22.5 °C. The scan rate is 0.1 V/s for both curves. (b) Plot of the total monolayer capacitance (C_T, obtained from cyclic voltammograms similar to those in Figure 1a) vs scan rate for an MUA monolayer in contact with a 1.0 M ionic strength electrolyte solution at pH = 2.04.

out of this solution, rinsed in pure ethanol, and attached to the ILIT cell (see Figure 3 of ref 24).

Before each ILIT experiment, the aqueous electrolyte solution contained either 0.10 or 1.00 M $NaClO_4$ along with 0.01 M H_3PO_4 which produced a pH of ~2.10. Cyclic voltammograms were performed on the MUA monolayers at this point in the experiment (Figure 1a). During the ILIT experiments, the pH of the electrolyte was varied by the addition of either 0.11 M NaOH (for the 0.10 M $NaClO_4$ solutions) or 0.11 M/0.89 M NaOH/$NaClO_4$ (for the 1.0 M $NaClO_4$ solutions). The ionic strength of these electrolyte solutions remained effectively constant (at either 0.10 or 1.0 M) as the pH was changed.[27] Also, during the course of these experiments, the pH of the electrolyte solutions was determined by removing a 0.5 mL aliquot of the solution from the ILIT cell and measuring the pH of this aliquot using an Orion model 601A meter equipped with an Orion model 910300 electrode. Basic electrolyte solutions were converted back to acidic solutions by the addition of 0.1 or 1.0 M perchloric acid solutions.

Johnson Matthey 99% pure (metals basis) $NaClO_4 \cdot H_2O$, Baker reagent grade phosphoric acid, Mallinckrodt reagent grade 2.0 N sodium hydroxide solution, and Baker Ultrex perchloric acid were all used as received to make the solutions used in this work. Water was purified in a Millipore Milli-Q Plus system. All ILIT experiments were performed at room temperature (23 ± 1 °C), and a saturated sodium calomel reference electrode (SSCE) was used in all experiments.[22]

Dielectric Saturation Effects in the Data Analysis. It was mentioned in the Introduction that dielectric saturation effects have to be considered in the calculation of the quantities C_{dl} and d ln $[C_{dl}]/dT$ (see eqs 4, 5, and 6). The theory of Grahame[23,28] was used to accomplish this. In this theory, the dependence of the electrolyte solvent dielectric constant (ϵ) on electric field strength (Φ) is given by[23,28]

$$\epsilon = \frac{(\epsilon_0 - n^2)}{[1 + (b/m)\Phi^2]^m} + n^2 \qquad (7)$$

where ϵ_o is the dielectric constant when Φ = O, $b = 1.2 \times 10^{-12}$ cm^2/V^2,[23,28] n is the optical refractive index of the solvent,[28] and m is determined to be 1.0 for water.[28] (Dielectric constants calculated with this value of m are equivalent to those determined by an alternative theory of dielectric saturation proposed by Booth.[29] Grahame's theory was used because it is mathematically simpler.)

If $\psi°$ is the potential of the outer Helmholtz plane (OHP) measured relative to the interior of the electrolyte solution, then[23]

$$\sinh^2\left(\frac{e\psi°}{2kT}\right) = \frac{D_0\int_0^{\Phi°}\epsilon\, d\Phi^2}{32\pi kTc_0} \qquad (8)$$

where k is Boltzmann constant, e is the electronic charge, $D_o = 1.1128 \times 10^{-12}$ coulomb/(V cm),[23] c_0 is the concentration of the electrolyte (molecules/cm^3), $\Phi°$ is the electric field strength at the OHP, and from eq 7

$$\int_0^{\Phi°}\epsilon\, d\Phi^2 = n^2\Phi°^2 + \frac{(D_0 - n^2)}{b}\ln[1 + b\Phi°^2] \qquad (9)$$

For a 1:1 electrolyte, the differential diffuse layer capacitance (C_{dl}^d) is given by

$$C_{dl}^d = \frac{4ec_0}{\Phi°}\left[\sinh^2\left(\frac{\epsilon\psi°}{2kT}\right)\left(1 + \sinh^2\left(\frac{\epsilon\psi°}{2kT}\right)\right)\right]^{1/2} \qquad (10)$$

where $\sinh^2(e\psi°/2kT)$ is calculated using eqs 8 and 9, and $\Phi°$ is determined by solving[23]

$$4\pi\nu_{dl}/D_0 = \int_0^{\Phi°}\epsilon\, d\Phi = n^2\Phi°^2 + \frac{(D_0 - n^2)}{\sqrt{b}}\tan^{-1}(\sqrt{b}\Phi°) \qquad (11)$$

for $\Phi°$. The quantity ν_{dl} in eq 11 is the excess charge per unit area in the entire diffuse double layer. As before (see eqs 3a and 3b), because C_{film} (and, consequently, C_T) ≪ C_{dl} at both ionic strengths investigated in the present study, ν_{dl} is assumed to be equal to $|\sigma_{A/B}|$. The integral double layer capacitance (C_{dl}) was obtained by numerically integrating C_{dl}^d as a function of ν_{dl}, and the quantity d ln C_{dl}/dT was determined by calculating ln $[C_{dl}]$ as a function of temperature and doing a numerical differentiation. Figures 2 and 3 contain plots of C_{dl} (Figure 2) and d ln $[C_{dl}]/dT$ (Figure 3) versus ν_{dl}. Included in these figures are plots of C_{dl} and d ln $[C_{dl}]/dT$ calculated using Gouy−Chapman theory with a constant dielectric constant. Note that there is a significant difference between the variable and constant dielectric constant plots beginning at ~1.5×10^{-5} couloumb/cm^2.

Results and Discussion

The cyclic voltammograms in Figure 1a are consistent with the expectation that there is an insulating layer of low dielectric

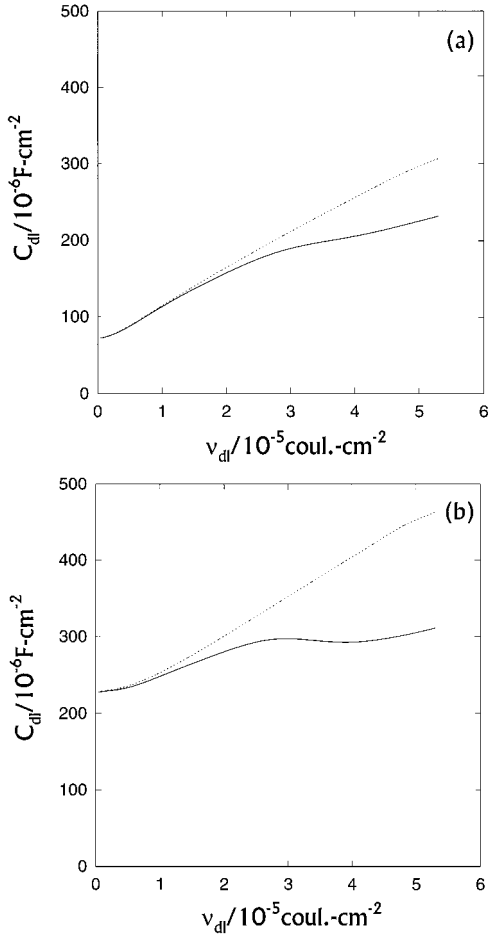

Figure 2. Plots of calculated (see the text) integral diffuse layer capacitance (C_{dl}) for aqueous 1:1 electrolyte solutions vs the excess charge per unit area in the entire diffuse double layer (ν_{dl}) at $T = 25$ °C. (a) Ionic strength = 0.10 M. (b) Ionic strength = 1.0 M. Dielectric saturation effects are included in the computation of the solid line curves (see eqs 7−11 in the text) while dielectric saturation effects were ignored in the calculation of the dotted line curves (i.e., the solvent (water) dielectric constant remained constant at 78.5).

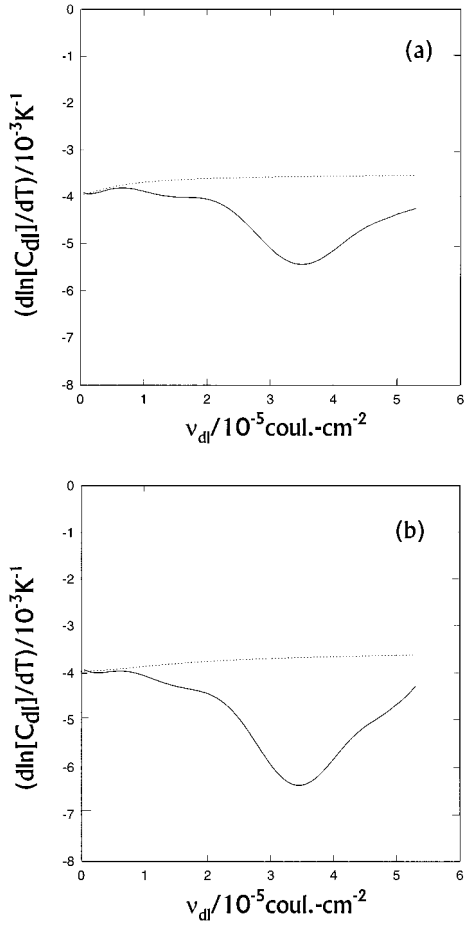

Figure 3. Plots of calculated d ln [C_{dl}]/dT for aqueous 1:1 electrolyte solutions vs ν_{dl} at $T = 25$ °C (see the text and Figure 2). (a) Ionic strength = 0.10 M. (b) Ionic strength = 1.0 M. Solid line curves: dielectric saturation effects included in the calculation. Dotted line curves: Dielectric saturation effects ignored in the calculation.

constant material between the gold electrode and the electrolyte solutions in the present experiments.[2] However, the charging currents at 1.0 M ionic strength are (mostly) larger than those at 0.10 M. Also, in a cyclic voltammetric experiment at 1.0 M ionic strength, the total monolayer capacitance (C_T) decreased as the scan rate increased (Figure 1b). The reason for these last observations is that the MUA monolayer is slightly permeable to ions resulting in a somewhat larger (low frequency) capacitance at the higher ionic strength.[2,30,31] These observations also indicate that the packing density for these MUA SAMs may be somewhat less than that expected for a perfect $(\sqrt{3}\times\sqrt{3})R30°$ overlay structure on Au(111) (i.e., 7.7×10^{-10} mol/cm^2).[2] (Chidsey and Loiacono[25] have found that MUA SAMs are quasi-liquids while SAMs composed of $HS(CH_2)_9CH_3$, $HS(CH_2)_{10}CH_2OH$, and $HS(CH_2)_{10}CN$ are all quasi-solid which suggests that interactions between adjacent terminal groups can effect the packing of a SAM.[2])

Figures 4 and 5 contain plots of the ILIT response (ΔV_t) at several applied potentials (E) measured at 0.10 M and 1.0 M ionic strength, respectively. There is a transient relaxation in several of these responses. These relaxations are well fit by[22,24]

$$\Delta V_t = A\Delta T_t^* + k_m B\int_0^t e^{-k_m(t-\tau)}\Delta T_\tau^* \, d\tau \qquad (12)$$

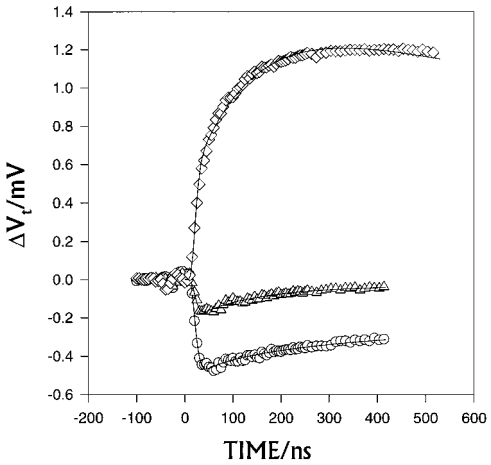

Figure 4. ILIT responses obtained from an Au electrode coated with an MUA monolayer: ionic strength = 0.10 M, pH = 2.16, $T = 23.9$ °C, $\Delta T_{eq} = 2.1$ °C. Circles: $E = 0$ mV vs SSCE; solid line curve describes a fit of these data to eq 12 for a purely thermal response ($B = 0$) with $A = -0.56$ mV. Triangles: $E = 200$ mV vs SSCE; solid line curve describes a fit of these data to eq 12 where $k_m = 6.1 \times 10^6$ s^{-1}, $A = -0.22$ mV and $B = 0.14$ mV. Diamonds: $E = 600$ mV vs SSCE; solid line curve describes a fit of these data to eq 12 where $k_m = 6.3 \times 10^6$ s^{-1}, $A = 0.66$ mV and $B = 1.46$ mV.

where $A\Delta T_t^*$ is the initial (open-circuit) potential response in the absence of any relaxation, $B\Delta T_t^*$ is the amplitude of the relaxation, and k_m is the measured first-order rate constant for

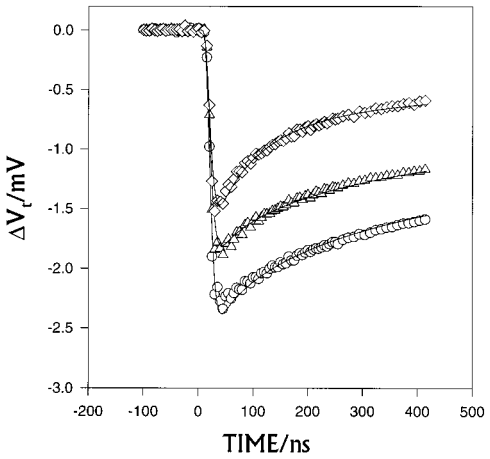

Figure 5. ILIT responses obtained from an Au electrode coated with an MUA monolayer: ionic strength = 1.0 M, pH = 6.11, T = 22.8°, ΔT_{eq} = 5.0 °C. Circles: E = −100 mV vs SSCE; solid line curve describes a fit of these data to eq 12 for a purely thermal response (B = 0) with A = −2.90 mV. Triangles: E = 200 mV vs SSCE; solid line curve describes a fit of these data to eq 12 for a purely thermal response (B = 0) with A = −2.21 mV. Diamonds: E = 400 mV vs SSCE; solid line curve describes a fit of these data to eq 12 where k_m = 1.0 × 10^7 s^{-1}, A = −1.92 mV and B = +0.72 mV.

the relaxation. ΔT_t^* is defined as

$$\Delta T_t^* = \Delta T_t/\Delta T_{eq} \qquad (13)$$

where ΔT_t is the interfacial temperature change at time t and ΔT_{eq} is the interfacial temperature change that would be produced if all the absorbed heat were uniformly distributed in the electrode and none of this heat were lost to either the dielectric "backing" material or the electrolyte solution. For $E \leq$ 200 mV versus SSCE at all pH's, the amplitude of the relaxation ($B\Delta T_t^*$) is quite small, in many cases being zero (see Figures 4 and 5). (When B = 0, the temporal dependence of the ILIT response follows that of the thermal perturbation.) For $E >$ 200 mV versus SSCE at all pH's the size of the relaxation increases as the potential increases until the relaxation accounts for most of the ILIT response. The measured value of the rate constant for the relaxation is independent of both applied potential and pH. However, the (average) value of k_m does vary with ionic strength, being (6.6 ± 1.6) × 10^6 s^{-1} at 0.10 M ionic strength and (1.2 ± 0.2) × 10^7 s^{-1} at 1.0 M ionic strength. The insensitivity of k_m to potential indicates to us that this ILIT relaxation is due to a (comparatively) slow relaxation of the MUA film's capacitance (C_{film}) in response to the temperature perturbation. This conclusion is consistent with the observation[25] that the MUA monolayer is quasi-liquid. Time-dependent changes in the monolayer dipole potential (V_D) cannot be the cause of the observed relaxation because the rates of these changes should be strong functions of potential, and the data in Figure 1b indicates that ions permeate into (or out) of an MUA monolayer on a time scale which is much slower than that associated with the ILIT technique.

Because the total response (defined as $\Delta E/\Delta T_{eq}$) of an electrode/electrolyte interface to the ILIT temperature perturbation is the sum of the quantities $A/\Delta T_{eq}$ and $B/\Delta T_{eq}$,[24] ΔE (in eq 2) is equal to ($A + B$). Figures 6 and 7 contain plots of $\Delta E/\Delta T_{eq}$ (see eq 2) versus potential (E) at 0.10 and 1.0 M ionic strengths, respectively. For all pH's studied at both ionic strengths, these plots are linear for $E \leq$ 200 mV versus SSCE, while for $E >$ 200 mV versus SSCE these plots all curve upward. However, well-defined potentials of zero response (E_{pzr}, see eq 3) may be obtained from the linear sections of these plots as the intercepts with the potential axis of lines such as those drawn in Figures 6 and 7. The slopes of these lines are equal to the quantity −d ln $[C_T]$/dT for this linear range of potential (i.e., −100 mV versus SSCE ≤ E ≤ 200 mV versus SSCE). Figures 8 and 9 contain plots of d ln $[C_T]$/dT for 0.10 and 1.0 M ionic strengths, respectively. For each of these plots, the different symbols refer to independent experiments on different monolayers.

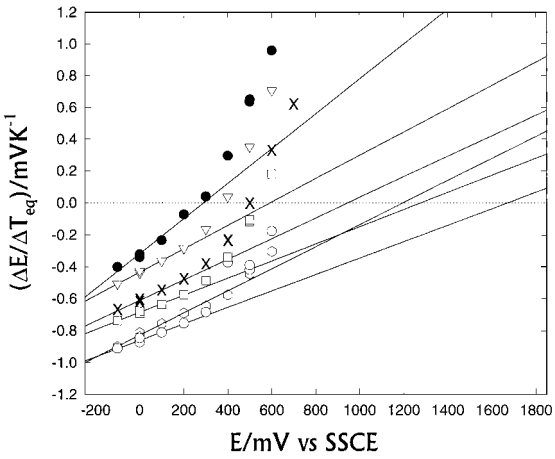

Figure 6. Plots of $\Delta E/\Delta T_{eq}$ (see the text) vs applied potential (E): ionic strength = 0.10 M, T = 23.7 °C. Filled circles: pH = 2.08. Triangles: pH = 3.48. ×'s: pH = 4.42. Squares: pH = 4.72. Open circles: pH = 5.61. Hexagons: pH = 8.37. Dotted line is at $\Delta E/\Delta T_{eq}$ = 0.

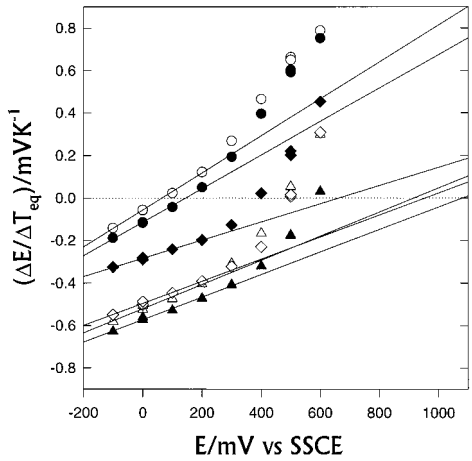

Figure 7. Plots of $\Delta E/\Delta T_{eq}$ (see the text) vs applied potential (E): ionic strength = 1.0 M, T = 22.2 °C. Open circles: pH = 2.07. Filled circles: pH = 2.84. Open triangles: pH = 5.38. Filled triangles: pH = 7.38. Open diamonds: pH = 7.70. Filled diamonds: pH = 9.37. Dotted line is at $\Delta E/\Delta T_{eq}$ = 0.

The first thing to note about the data plotted in Figures 8 and 9 is that the reproducibility from experiment to experiment (monolayer to monolayer) is quite good. This not only validates our procedures for making these monolayers, but also our technique for measuring ΔT.[22] The data in Figures 8 and 9 (as well as the values of the relaxation rate constant) are independent of the potential history and the pH history of the MUA monolayer. That is, at a particular pH, the order of the potentials (E) at which the ILIT experiments are performed does not matter, and, at a particular potential, the same results are obtained no matter whether the monolayer had previously been in its acid form or basic form.

The other thing to note about the data plotted in Figures 8 and 9 is that the absolute value of d ln $[C_T]$/dT decreases with

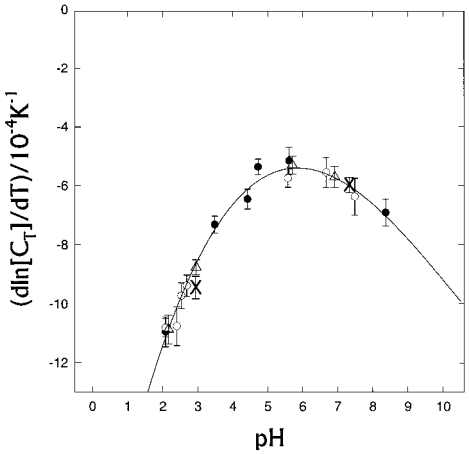

Figure 8. Plots of d ln $[C_T]$/dT (see eq 2) vs pH: ionic strength = 0.10 M. The different symbols refer to independent experiments on separate MUA monolayers. The ×'s refer to the experiment performed when 1.0×10^{-3} M of Ca^{2+} was added to the electrolyte solution. The curve describes a third power polynomial fit to the data. This curve has no theoretical significance.

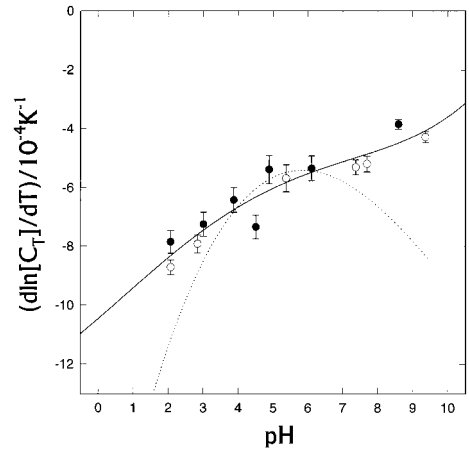

Figure 9. Plots of d ln $[C_T]$/dT (see eq 5) vs pH: ionic strength = 1.0 M. The different symbols refer to independent experiments on separate MUA monolayers. The solid line curve describes a fourth power polynomial fit to the data. This curve has no theoretical significance. The dotted line curve is the third power polynomial fit from Figure 8.

increasing pH for pH's less than 7.0 at 0.10 M ionic strength and for all pH's studied at 1.0 M ionic strength. An explanation for this behavior would require detailed information concerning the structure of these monolayers as a function of temperature and pH (e.g., we would need to know how temperature and pH affect the tilt angle[1,2] of the alkane chains and if or how the acidic hydrogen forms hydrogen bonds[31,32]). Because the ILIT technique does not provide such information, such an explanation is, therefore, beyond the scope of this work. The only things we can say on this subject at present is to point out that the values of d ln $[C_T]$/dT at low pH are approximately the same as d ln $[\epsilon_H]$/dT, where ϵ_H is the dielectric constant of a normal-alkane hydrocarbon (e.g., d ln $[\epsilon_H]$/d$T = -9.2 \times 10^{-4}$ K^{-1} for undecane)[33] and that the average d ln $[C_T]$/dT for pH's greater than 6.5 at both ionic strengths is approximately the same as the value of d ln $[C_T]$/dT obtained for an undecanethiol monolayer in contact with 1.0 M $HClO_4$ (i.e., $(-5.8 \pm 0.5) \times 10^{-4}$ K^{-1}).

Figure 10a contains a plot (the open circles) of E_{pzr} versus pH measured at 0.10 M ionic strength. The size of the error bars in Figure 10a (as well as in Figure 11) is mainly determined by the length of the extrapolation needed to obtain E_{pzr}. The

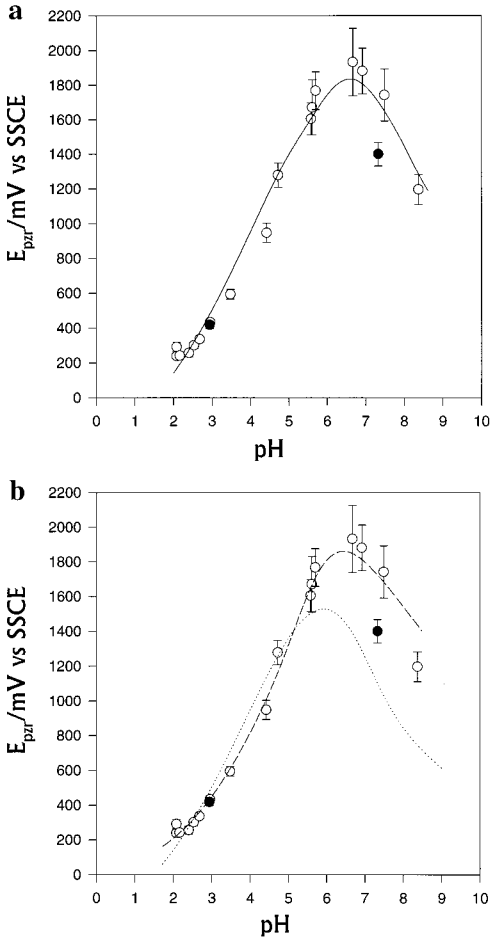

Figure 10. Plots of E_{pzr} (see eq 5) vs pH: ionic strength = 0.10 M. (a) Open circles: no Ca^{2+} added to the electrolyte solution. Filled circles: 1.0×10^{-3} M Ca^{2+} added to the electrolyte solution. Curve: fit of the open circle data to eqs 4, 5 and 6 (see Table 1). (b) Open circles: no Ca^{2+} added to the electrolyte solution. Dotted line curve: calculated using the parameters in Table 1 for ionic strength = 0.10 M but without including dielectric saturation effects in the calculation of C_{dl} and d ln $[C_T]$/dT. Dashed line curve: fit of the (open circle) data to eqs 4, 5, and 6 resulting when dielectric saturation effects are ignored in the calculation of C_{dl} and d ln $[C_T]$/dT. This fit gives pK_a = 3.8, pK_∞ = 1.1, $\Gamma_T = 8.6 \times 10^{-10}$ mol/cm^2, dV_D/d$T = -0.55$ mV/K, $V_D = -130$ mV vs SSCE and d ln K_∞/d$T = -2.0 \times 10^{-2}$ K^{-1}.

curve in Figure 10a is a fit of these data to eqs 4, 5, and 6 resulting in pK_a = 5.7 and $\Gamma_T = 5.5 \times 10^{-10}$ mol/cm^2 for this ionic strength (see Table 1). The same data is plotted in Figure 10b, and the dotted curve in this figure is calculated using the parameters in Table 1 for ionic strength 0.10 M but without including dielectric saturation effects in the calculation of C_{dl} and d ln $[C_{dl}]$/dT (see eqs 4, 5, and 6). This dotted curve fits the data in Figure 10b poorly for pH's < 5.0, and, for pH's > 5.0, it does not fit these data at all. The dashed curve in Figure 10b represents the best fit of the E_{pzr} data to eqs 4, 5, and 6 when the effects of dielectric saturation are ignored. There are two reasons why we do not consider the results obtained from the fit described by this dashed curve to be valid. First, although the fit associated with this dashed curve is approximately as good as the fit obtained when dielectric saturation effects are included, the Γ_T ($= 8.6 \times 10^{-10}$ mol/cm^2) obtained from the fit in Figure 10b is greater than that expected[2,34] for a densely packed $(\sqrt{3}\times\sqrt{3})R30°$ structured monolayer on Au(111).[35] Our cyclic voltammetric results (as well as the results of Chidsey and Loiacono[25]) indicate that the MUA monolayers are not densely packed, i.e., the surface coverage of these monolayers

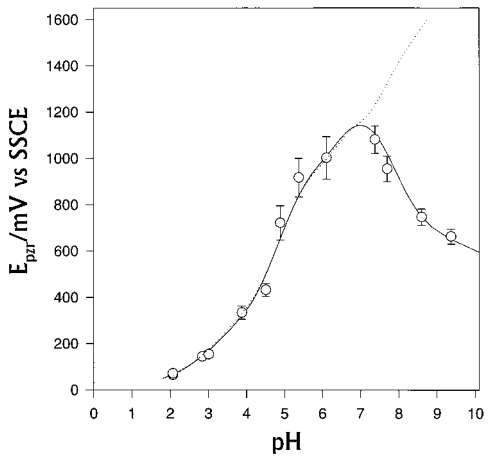

Figure 11. Plot of E_{pzr} (see eq 3) vs pH: ionic strength = 1.0 M. Dotted line curve: fit of the data for pH's < 6.5 to eqs 4, 5, and 6 (see Table 1). Solid line curve: fit of all of these data to eqs 4, 6, and 14 (see Table 1).

TABLE 1: Results from the Fits of the E_{pzr} versus pH Data[a,b]

ionic strength/M	0.10	1.0	
pK_a	5.7 ± 0.2^d	$4.5 \pm 0.2^{d,e}$	4.4 ± 0.2^f
pK_∞[c]	3.2 ± 0.2^d	$3.0 \pm 0.2^{d,e}$	2.9 ± 0.2^f
$\Gamma_T/(\times 10^{-10}$ mol/cm^2)	5.5 ± 0.3^d	$5.5 \pm 0.3^{d,e}$	5.2 ± 0.3^f
V_D/mV vs SSCE	-280 ± 110^d	$99 \pm 69^{d,e}$	83 ± 65^f
$(dV_D/dT)/$(mV/K)	-0.22 ± 0.14^d	$0.11 \pm 0.06^{d,e}$	0.07 ± 0.04^f
(d ln $K_\infty/dT)/10^{-2}$ K^{-1}	1.9 ± 1.2	$0.3 \pm 0.6^{d,e}$	0.1 ± 0.6^f

[a] See Figures 10a and 11. [b] Dielectric saturation effects included in the calculation of C_{dl} and d ln $[C_{dl}]/dT$. [c] See eq 4. [d] Fitted to eqs 4, 5, and 6. [e] Fit limited to data at pH's < 6.5 (dotted line curve in Figure 11). [f] From fit of the entire data set at 1.0 M ionic strength to eqs 4, 6, and 14, where $K_M = (1.8 \pm 0.7) \times 10^6$ M^{-1}, $V_{C,D} = 870 \pm 300$ mV vs SSCE and $dV_{C,D}/dT = 0.10 \pm 0.06$ mV/K.

should be less than optimum which is the result obtained from the fit in Figure 10a.[36] Second, and more importantly, it is not physically reasonable to ignore dielectric saturation in the analysis of this E_{pzr} data.

Li and co-workers[5] have found that a number of cations (i.e, Cd^{2+}, Pb^{2+}, Ba^{2+}, and Ca^{2+}) form counterion overlayers at the interface between an electrolyte solution containing the cation and a monolayer composed of an ω-carboxylic alkanethiols self-assembled on gold. These cations complex with the dissociated carboxylic acid moiety at high pH, i.e., OH^- coadsorbs with the divalent cations mentioned in the preceding sentence.[5] The filled circles in Figure 10a demonstrate the effect (on E_{pzr}) of adding 1.0×10^{-3} M Ca^{2+} ion to a 0.10 M ionic strength electrolyte solution in contact with an MUA monolayer. At low pH (= 2.97), the presence of the Ca^{2+} ion has no effect on E_{pzr}, but at pH = 7.33 this concentration of Ca^{2+} ion causes a small but definite decrease in the value of E_{pzr}. (The values of d ln $[C_T]/dT$ at both pH's are uneffected by the presence of Ca^{2+}; see Figure 8). These results are consistent with the observations of Li and co-workers;[5] that is, the Ca^{2+} ion does not interact with $-$COOH, but, when these carboxylic acid moieties are dissociated, the Ca^{2+} (and OH^-)[5] ions complex with them, thereby modifying the electric field at the monolayer/electrolyte interface and changing E_{pzr}.

The possible formation of a counterion overlayer involving Ca^{2+} is a significant issue for the analysis of the experiments at 1.0 M ionic strength because the Johnson Matthey $NaClO_4 \cdot H_2O$ used in these experiments contained a very small amount of calcium as an impurity.[38] (Cadmium and barium are not present in this salt, and lead is present in insufficient quantity to be of importance.[38]) Accordingly, the first fit (to eqs 4, 5, and 6) of the E_{pzr} data obtained from the experiments at 1.0 M ionic strength (plotted in Figure 11) was limited to the data taken at pH's <6.5. The dotted curve in Figure 11 demonstrates that this fit is a good representation of the 1.0 M ionic strength data up to pH = 6.5. For pH > 7.5, there is a precipitous decrease in E_{pzr} which is not described by the extrapolation of this first fit, and which is probably due to the formation of a counterion overlayer involving Ca^{2+} (and OH^-) ions. The complete data set in Figure 11 was, therefore, fit to

$$E_{pzr} = \left\{\left[V_D + \frac{dV_D/dT}{d\ln[C_T/dT]} - \frac{\sigma_{A/B}}{C_{dl}}\left(\frac{d\ln[C_{dl}]/dT}{d\ln[C_T]/dT} - 1 - \frac{d\ln K_D/dT}{d\ln[C_T]/dT}\left(\frac{[H^+]}{[H^+]+K_D}\right)\right)\right] + K_M[OH^-]\left(V_{C,D} + \frac{dV_{C,D}/dT}{d\ln[C_T]/dT}\right)\right\}/(1 + K_M[OH^-]) \quad (14)$$

where $V_{C,D}$ and $dV_{C,D}/dT$ are the dipole potential and its temperature derivative for an MUA monolayer covered with the Ca^{2+}/OH^- complex counterion overlayer, and K_M is the equilibrium constant for the formation of this complex. Equation 14 describes the behavior of E_{pzr} when log $[K_M] < (14 - pK_a)$. The solid curve in Figure 11 shows that the fit of all of the data obtained at 1.0 M ionic strength to eq 14 (and eqs 4 and 6) is a very good representation of these data. Furthermore, the values of Γ_T, pK_a, pK_∞, V_D, d ln K_∞/dT, and dV_D/dT obtained from the fit to eq 14 (see Table 1) are the same (within experimental error) as those obtained from the fit which was limited to the data taken at pH's < 6.5. The value of $dV_{C,D}/dT$ is also essentially the same as that of dV_D/dT (from either fit) while $V_{C,D}$ is considerably different from V_D (also from either fit). The equivalency of dV_D/dT and $dV_{C,D}/dT$ is consistent with the conclusion that these quantities are both due to interactions within the first layer of the MUA monolayer (the layer between the gold electrode and the ionizable functional group[14]) so that they are uneffected by the formation of the counterion overlayer. On the other hand, the big difference between V_D and $V_{C,D}$ is consistent with the expectation that a counterion overlayer complex between three separate ionic species ($-COO^-$, OH^-, and Ca^{2+}) should have a significant dipole moment[39] which will have a large effect on the dipole potential associated with the MUA monolayer.

The error bounds reported in Table 1 come from a statistical analysis of the fits in Figures 10 and 11. An important point to come out of this statistical analysis is that, because the values of C_{dl} and d ln $[C_{dl}]/dT$ may be fixed by diffuse double layer theory, the fitted curves in these figures depend mostly on the values of Γ_T and pK_a (which is, in turn, dependent upon the value of pK_∞). This point is demonstrated by the large errors (relative to the reported values) given for V_D, dV_D/dT, and d ln K_D/dT in Table 1 in comparison to the relative errors reported for Γ_T and pK_a (and pK_∞). Accordingly, the agreement between the values of Γ_T determined at both ionic strengths studied (see Table 1) must be emphasized. Because all of the monolayers studied were formed in ethanol solutions containing only MUA, the value of Γ_T determined from the analysis of the E_{pzr} versus pH data should be independent of ionic strength which is what we observe. This agreement between the values of Γ_T determined at different ionic strengths is not only a validation of our use of the simplified equation for the calculation of K_D (eq 3b) and our procedure for computing C_{dl} and d ln $[C_{dl}]/dT$ but also verifies an assumption which is implicit in our analysis of

the E_{pzr} data that the values of V_D and dV_D/dT are not functions of pH. The result that the values of both V_D and dV_D/dT are different at the two ionic strengths investigated (even when the combination of the two error bounds at the two ionic strengths are considered for these quantities; see Table 1) is also consistent with the observation that the values of E_{pzr} determined at low pH's (i.e., pH < 3.0) are different for the two ionic strengths (see Figures 10 and 11). Because E_{pzr} depends only on V_D, dV_D/dT, and $d \ln [C_T]/dT$ when $\sigma_{A/B} \rightarrow 0$ (i.e., when pH $\ll$ pK_a) and the differences between the values of $d \ln [C_T]/dT$ measured at the two ionic strengths for pH's < 3.0 are in the wrong direction to cause the observed variation in E_{pzr} at these pH's, both V_D and dV_D/dT must be different at the different ionic strengths. Table 1 also contains the values determined for $d \ln K_\infty/dT$. All three of the values reported for this quantity are small and may reasonably be surmised to be the same within experimental error.

It is also of interest to investigate whether the pK_a of an MUA monolayer varies with electrode potential. It has already been mentioned in the Introduction that a linear plot of $\Delta E/\Delta T_{eq}$ versus applied electrode potential can only be obtained if pK_a is independent of potential. The pK_a of an MUA monolayer, therefore, does not vary with applied electrode potential in the range of −100 to +200 mV versus SSCE. However, the curvature observed in the plots of $\Delta E/\Delta T_{eq}$ versus potential for E > 200 mV versus SSCE (see Figures 6 and 7) does not necessarily mean that pK_a varies with potential because potential variation in several other quantities (i.e., $d \ln [C_T]/dT$, $d \ln [C_{dl}]/dT$, C_{dl}, V_D, $d \ln K_\infty/dT$, and dV_D/dT) may also cause this curvature. Also, because the behavior of a number of quantities may be responsible for the curvature in the plots of $\Delta E/\Delta T_{eq}$ versus E when E > 200 mV versus SSCE, the slopes of these plots in this potential range are not necessarily equal to $d \ln [C_T]/dT$.[42] Accordingly, the variation of pK_a with applied potential was investigated by plotting $\Delta E/\Delta T_{eq}$ measured at particular E as a function of pH and observing whether these plots have clearly defined plateau regions which may be attributed to the acid and basic forms of the carboxylic acid moiety in the MUA monolayer. Such plots are shown in Figure 12 for E = 600 mV versus SSCE (12a) and E = −100 mV versus SSCE (12b) at 0.10 M ionic strength. Although there is considerable scatter in the data (especially in Figure 12b), both of these plots demonstrate acidic and basic plateau regions, and the pK_a at each of these potentials may be defined as the pH at the midpoint (on the $\Delta E/\Delta T_{eq}$ axis) between the acidic and basic plateaus (see the arrows in Figure 12, a and b). At E = 600 mV vs SSCE, this pK_a (4.6 ± 0.5) is somewhat lower than that reported in Table 1, but, at E = −100 mV vs SSCE, the pK_a determined from the data in Figure 12b (4.2 ± 0.6) is even lower (although this latter pK_a is within experimental error of that determined at 600 mV vs SSCE). It, therefore, may be surmised that an analysis such as that just described for the data in Figure 12a,b produces values of pK_a which are uniformly lower (by as much as 1.5pH unit) than those determined from an analysis of E_{pzr} data and that the pK_a of a MUA monolayer is not a function of potential for E > 200 mV vs SSCE (which also means that pK_a is not a function of σ_M, see eq 1). The first observation in the preceding sentence is easily explained by noting (see eq 2) that the proportionality between ΔE (measured at a particular potential) and the fraction of the carboxylic acid moieties which are dissociated (i.e., $\sigma_{A/B}$) is a function of potential. So, a difference between the value of pK_a determined from a plot such as those in Figure 12 and that determined from a fit to eqs 4, 5, and 6 should be expected. That this difference remains substantially the same at all potentials up to 600 mV vs SSCE is at present only a supposition. (The pK_a's determined through plots such as those in Figure 12 at other potentials ≤200 mV vs SSCE are essentially the same as that determined through the plot in Figure 12a, but this does not necessarily mean that the difference between pK_a's determined through this technique and the actual pK_a's remain the same for potentials >200 mV vs SSCE.) Therefore, it must be emphasized that our statement concerning the variation pK_a with potential (for E >200 mV vs SSCE) is just an inference and not, as yet, a definite conclusion.

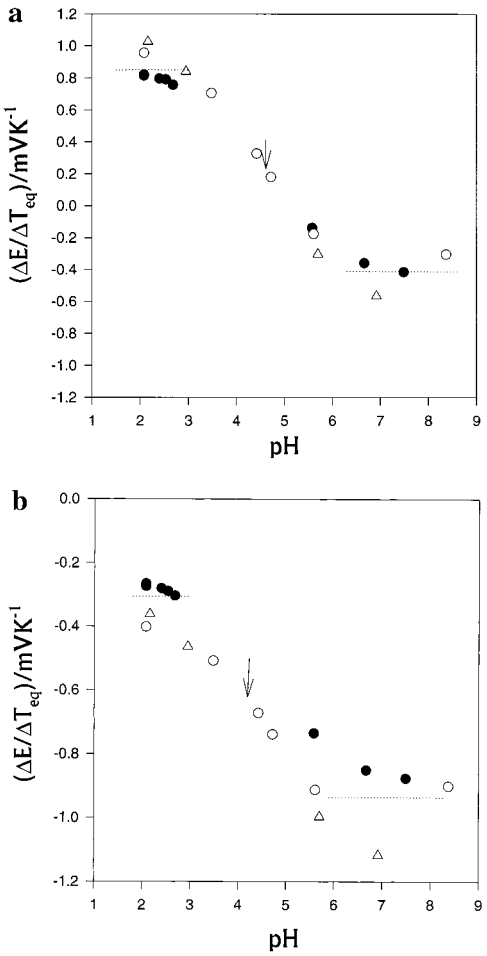

Figure 12. Plots of $\Delta E/\Delta T_{eq}$ vs pH: ionic strength = 0.10 M. The dotted lines signify the acidic and basic plateau regions determined for these plots, and the arrows signify the pK_a's determined from the technique based on these plots. (a) Applied potential = 600 mV vs SSCE, pK_a = 4.6 ± 0.5. (b) Applied potential = −100 mV vs SSCE, pK_a = 4.2 ± 0.6. The different symbols refer to independent experiments on separate MUA monolayers.

Conclusions

Combining the values of pK_a given in Table 1 with that reported by Creager and Clarke[3] (for MUA, pK_a = 6.4 at an ionic strength of 1.3×10^{-2} M)[43] and that reported by Hu and Bard[44] (for 3-mercaptopropionic acid, pK_a = 7.7 at an ionic strength of ca. 1.0×10^{-3} M) demonstrates a consistent decrease in pK_a with increasing ionic strength. The reason for this behavior is quite simply that, for a particular value of $\sigma_{A/B}$, the magnitude of the interfacial potential at the monolayer surface (i.e., the diffuse double layer potential) becomes smaller as the ionic strength of the electrolyte solution increases. In other words, the Coulombic attraction between the hydrogen cations in the solution and the carboxylate anions on the surface of the monolayer is a decreasing function of ionic strength so that the

carboxylic acid moiety becomes a stronger acid when the ionic strength of the electrolyte solution in contact with the monolayer increases. This interfacial potential effect has often been used to explain shifts in the pK_a's of acids adsorbed on charged interfaces such as those which exist on micelles and liquid monolayers or bilayers.[3,45−47] Additionally, this explanation for the effect which the electrolyte solution ionic strength has on the pK_a of an MUA monolayer is strengthened by our observation (see Table 1) that the value of pK_∞ is insensitive to ionic strength, i.e., when diffuse double layer effects (and, thereby, interfacial potential effects) are removed from the acid dissociation constant of the carboxylic acid moiety (K_D), the resulting equilibrium constant (K_∞) is not a function of ionic strength.

In homogeneous solutions having ionic strengths which are less than or equal to 1.0 M, the pK_a's of alkane carboxylic acids are relatively insensitive to ionic strength. For example at an ionic strength of 0.01 M, the pK_a of acetic acid in a $NaClO_4$ electrolyte solution[48] is 4.68; at 0.10 M, this pK_a = 4.60; and, at 1.0 M, this pK_a = 4.64. Additionally, at ionic strengths which are greater than 1.0 M, the pK_a's of these acids increase with increasing ionic strength (for example, the pK_a of acetic acid in 2.5 M $NaClO_4$ is 4.94[48]). These observations not only are additional evidence that the variation of the pK_a of an MUA monolayer with ionic strength is due to the interfacial potential effect discussed in the preceding paragraph (i.e., the dissociation reaction of the carboxylic acid moiety has to take place across an interface to cause this variation), but also they demonstrate that the microenvironment at the monolayer interface either stabilizes the carboxylate anion and/or makes the carboxyl proton more acidic (because our measured value of pK_∞ (for the interfacial reaction) is considerably less than the values of pK_a determined for the homogeneous solution reaction at high ionic strengths[48] ($\gg$1.0 M)).

One possible origin for a putative stabilization of the carboxylate anion at the monolayer interface is the image charge interactions which arise from the fact that the charges on these anions are discrete[49−53] and are, therefore, not smeared out over the entire monolayer/solution interface as well as from the fact that these charge are bound to a very high dielectric medium (the gold electrode) by a very low dielectric constant medium (the monolayer up to the PAD). However, calculations based upon the three phase (i.e., solution/film/electrode) model for the image charge interactions of an ion present on the solution side of an interface with a film-coated electrode which has been proposed by Liu and Newton[54] demonstrate that the stabilization (i.e., negative change in the free energy for the hydrogen ion dissociation reaction (ΔG_r)) effected by these image charge interactions is not strong enough to overcome the positive change in ΔG_r caused by transferring the carboxylate anions from a high dielectric constant medium (an aqueous electrolyte solution) to a relatively low dielectric constant medium (the MUA monolayer/electrolyte solution interface).[3] The Liu and Newton model only determines self-imaging interactions[54] of isolated ions.[41,51] Image interactions involving neighboring carboxylate ions are, consequently, ignored. This was done in order to be consistent with both our experimental results and an (implicit) assumption underlying the analysis of these results. That is, in order for eqs 3 and 4 to be valid, the free energy of reaction (ΔG_r) cannot be a function of $\sigma_{A/B}$. Also, if there were significant interactions between the neighboring carboxylate ions, pK_a should be dependent upon potential.[41] We have already commented upon the apparent lack of dependence of pK_a upon potential and an analysis of the experimental results based upon eq 4 gives an excellent representation of these data. We, therefore, conclude that image interactions between neighboring carboxylate ions are negligible so that these interactions cannot be the cause of a stabilization of the carboxylate ion at the monolayer/electrolyte solution interface.

The possibility that the carboxyl proton is more acidic at the monolayer interface may originate from the known[55] difference in stability of the syn (O−H and C═O on the same side of C−O) and anti (O−H and C═O on opposite sides of C−O) conformations of the carboxyl moiety. The syn conformation is the more stable form, so that[56]

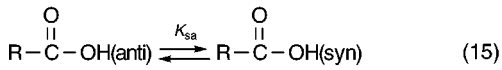

(15)

where K_{sa} is approximately 10.[4] If the microenvironment at the monolayer interface forces the carboxyl moiety into the anti conformation, then the carboxyl proton will be acidic than in solution (where the syn conformation is the dominant form). There is simply too much uncertainty in the models for this interface at present[2,57] to make a definitive statement on the origin of any factors which may force the carboxyl moiety into the anti conformation. Nevertheless, a combination of the negative ΔG_r caused by image charge interactions with the (possible) ΔG_r caused by the syn/anti conformational effects just discussed may be strong enough to overcome the positive ΔG_r caused by transferring the carboxylate anion from the aqueous electrolyte solution to the monolayer/solution interface. Such a combination, thereby, may explain our observation that pK_∞ (for the interfacial reaction) is considerably less than the values of pK_a measured in high ionic strength aqueous solutions.

In the present study, we have demonstrated that the simplified model of Smith and White[13,14] provides a very good basis for the analysis of E_{pzr} vs pH data obtained from ILIT experiments on Au electrodes coated with self-assembled monolayers of an ω-carboxylic acid substituted alkanethiol. There have been improvements suggested for this rather basic model. For example, Fawcett and co-workers have proposed a three-layer model for the monolayer/electrolyte interface.[2,41,49,50] The first layer in this model contains the monolayer up to the ionizable functional group (i.e., the low dielectric constant, hydrocarbon domain of the monolayer up to the PAD), the second layer contains this functional group and ends at the outer Helmholtz plane (OHP, i.e., the closest distance of approach of solvated counterions), and the third layer begins at the OHP and extends into the bulk of the electrolyte solution. (Discreteness of charge effects are also included in this model.) For simplicity, Fawcett and co-workers have assumed that the dielectric constant of the second layer is the same as that of the first layer. This is certainly an oversimplification which can only be improved upon by including a variation of the dielectric constant with distance (from the PAD) in the model used to describe the monolayer/electrolyte interface. This is equivalent to what we have done by including dielectric saturation effects into the simple, two-layer model of Smith and White so that this latter model may be a better representation of the monolayer/electrolyte solution interface than might be expected due to its simplicity.

Despite possible uncertainties about the proper model to use to analyze the data presented in this paper, it must be emphasized that these uncertainties raise questions of interpretation and not of observation—at both ionic strengths studied, E_{pzr} does vary with pH in a manner consistent with the occurrence of a hydrogen ion dissociation reaction at the monolayer/electrolyte solution interface. The present study, therefore, is a further demonstration[24] that ILIT the technique, which was originally

developed to study the dynamics of fast interfacial charge-transfer reactions,[24] can also provide information on the structure of charges at an electrode/solution interface and, consequently, the thermodynamics of these reactions.

Acknowledgment. J.F.S., K.C., and S.W.F. gratefully acknowledge the support of the Chemical Sciences Division, Office of Basic Energy Sciences, U.S. Department of Energy Contract No. DE-AC02-98CH10086. J.F.S. and S.W.F. acknowledge many helpful discussions with Dr. Marshall D. Newton, Chemistry Department, Brookhaven National Laboratory. The authors would also like to thank Prof. Christopher E.D. Chidsey and Ms. Sandra B. Sachs (Chemistry Department, Stanford University) for making the gold film electrodes used in this work.

References and Notes

(1) Dubois, L. H.; Nuzzo, R. G. *Annu. Rev. Phys. Chem.* **1992**, *43*, 437.

(2) Finklea, H. O. In *Electroanalytical Chemistry*, Bard, A. J., Rubinstein, I., Eds.; Marcel Dekker: New York, 1996; pp 109−335; Vol. 19.

(3) Creager, S. E.; Clarke, J. *Langmuir* **1994**, *10*, 3675.

(4) Scarlata, S. F.; Rosenberg, M. *Biochemistry* **1990**, *29*, 10233.

(5) Li, J.; Lang, K. S.; Scoles, G.; Ulman, A. *Langmuir* **1995**, *11*, 4418.

(6) Song, S.; Clarke, R. A.; Bowden, E. F. *J. Phys. Chem.* **1993**, *97*, 6564.

(7) Feng, Z. Q.; Imabayashi, S.; Kakuichi, T.; Niki, K. *J. Electroanal. Chem.* **1995**, *394*, 149.

(8) Nahir, T. M.; Bowden, E. F. *J. Electroanal. Chem.* **1996**, *410*, 9.

(9) Bain, C. D.; Whitesides, G. M. *Langmuir* **1989**, *5*, 1370.

(10) Lee, T. R.; Carey, R. D.; Biebuyck, H. A.; Whitesides, G. M. *Langmuir* **1994**, *10*, 741.

(11) Wang, J.; Frostman, L. M.; Ward, M. D. *J. Phys. Chem.* **1992**, *96*, 5224.

(12) (a) Bryant, M. A.; Crooks, R. M. *Langmuir* **1993**, *9*, 385. (b) White, H. S.; Peterson, J. D.; Cui, Q.; Stevenson, K. J. *J. Phys. Chem. B* **1998**, *102*, 2930.

(13) Smith, C. P.; White, H. S. *Anal. Chem.* **1992**, *64*, 2398.

(14) Smith, C. P.; White, H. S. *Langmuir* **1993**, *9*, 1.

(15) Mullen, K. I.; Wang, D.; Crane, L. G.; Carron, K. T. *Anal. Chem.* **1992**, *64*, 930.

(16) Eisenthal, K. B. *Acc. Chem. Res.* **1993**, *26*, 636.

(17) Zhao, X.; Ong, S.; Wang, H.; Eisenthal, K. B. *Chem. Phys. Lett.* **1993**, *214*, 203.

(18) Yan, E. C. Y.; Liu, Y.; Eisenthal, B. *J. Phys. Chem. B* **1998**, *102*, 6331.

(19) Smalley, J. F.; Krishnan, C. V.; Goldman, M.; Feldberg, S. W. *J. Electroanal. Chem.* **1988**, *248*, 255.

(20) Smalley, J. F.; MacFarquhar, R. A., Feldberg, S. W. *J. Electroanal. Chem.* **1988**, *256*, 21.

(21) Bard, A. J.; Faulkner, L. R. *Electrochemical Methods: Fundamentals and Applications*; John Wiley & Sons: New York, 1980; p 507.

(22) Smalley, J. F.; Feldberg, S. W.; Chidsey, C. E. D.; Linford, M. R.; Newton, M. D.; Liu, Y.-P. *J. Phys. Chem.* **1995**, *99*, 13141.

(23) Grahame, D. C. *J. Chem. Phys.* **1950**, *18*, 903.

(24) Smalley, J. F.; Geng, L.; Rogers, L.; Feldberg, S. W.; Leddy, J. *J. Electroanal. Chem.* **1993**, *356*, 181.

(25) Chidsey, C. E. D.; Loiacono, D. *Langmuir* **1990**, *6*, 682 and references therein.

(26) Bain, C. D.; Troughton, E. B.; Tao, Y.-T.; Evall, J.; Whitesides, G. M.; Nuzzo, R. G. *J. Am. Chem. Soc.* **1989**, *111*, 321. See Supporting Information accompanying this reference for synthetic procedures.

(27) For example, the average ionic strength of the nominally 0.100 M ionic strength solutions is 0.103 ± 0.004 M.

(28) Grahame, D. C. *J. Chem. Phys.* **1953**, *21*, 1054.

(29) Booth, F. *J. Chem. Phys.* **1951**, *19*, 391.

(30) Porter, M. D.; Bright, T. B.; Allara, D. L.; Chidsey, C. E. D. *J. Am. Chem. Soc.* **1987**, *109*, 3559.

(31) Rebek, J., Jr.; Duff, R. J.; Gordon, W. E.; Parris, K. *J. Am. Chem. Soc.* **1986**, *108*, 6068.

(32) Nuzzo, R. G.; Dubois, L. H.; Allara, D. L. *J. Am. Chem. Soc.* **1990**, *112*, 558.

(33) Weast, R. C., Ed. *Handbook of Chemistry and Physics*; CRC Press: Cleveland, OH, 1966; p E-56.

(34) Zhang, C.-J.; Porter, M. D. *J. Am. Chem. Soc.* **1994**, *116*, 11616.

(35) Chidsey, C. E. D.; Liu, G.-Y.; Rowntree, P.; Scoles, G. J. L. *J. Chem. Phys.* **1989**, *91*, 4421.

(36) Reductive desorption in aqueous 0.5 M KOH[37] was used in an attempt to determine the surface coverage of the MUA monolayers investigated here independently of the ILIT experiments. This attempt failed because no voltammetric peak was observed positive of solvent reduction.

(37) Widrig, C. A.; Chung, C.; Porter, M. D. *J. Electroanal. Chem.* **1991**, *310*, 335.

(38) This information is obtained from the certificate of analysis of the $NaClO_4 \cdot H_2O$ used (private communication from: Valerie Kennedy, Johnson Matthey, Alfar Aesar, 30 Bond St., Ward Hill, MA). From this certificate of analysis, the maximum concentration of Ca^{2+} ion in a 1.0 M solution made from this $NaClO_4 \cdot H_2O$ is 3.5×10^{-4} M.

(39) The difference (ΔV_u) between $V_{C,D}$ and V_D (i.e., the change in the dipole potential presumably caused by the formation of the counterion overlayer complex) is 0.77 V (see the results obtained from the fit of the entire 1.0 M ionic strength data set in Table 1). The perpendicular component of the dipole moment ($\mu_\perp$) associated with this change in the dipole potential may be calculated from[40] $\mu_\perp = \Delta V_u \epsilon_C \epsilon_O M_A$, where M_A is the surface area associated with the component molecules of the monolayer, ϵ_C is the average relative permittivity of the part of the diffuse layer containing the counterion overlayer complex, and ϵ_0 is the permittivity of free space. For $\Gamma_T = 5.4 \times 10^{-10}$ mol/cm^2 (see Table 1), $M_A = 3.1 \times 10^{-15}$ cm^2/molecule, and, if it is assumed[41] that $\epsilon_C = 3.0$, then $\mu_\perp = 1.9$ D which is a very reasonable value for a complex composed of ionic species.

(40) Evans, S. D.; Urankar, E.; Ulman, A.; Ferris, N. *J. Am. Chem. Soc.* **1991**, *113*, 4121.

(41) Andreu, R.; Fawcett, W. R. *J. Phys. Chem.* **1994**, *98*, 12753.

(42) If the apparent correlation between the size of the ILIT relaxation ($B\Delta T_t^*$, see Figures 4 and 5) and applied potential when $E > 200$ mV vs SSCE is combined with our earlier conclusion that this relaxation is due to a comparatively slow response of the film's capacitance to the temperature perturbation, d ln C_T/dT (see eq 2) may very well become a strong function of potential at positive potentials thereby causing the curvature in the plots such as those in Figures 6 and 7 at these potentials. However, because the total response ($\Delta E/\Delta T_{eq}$) to the ILIT perturbation depends on both A and B, and A is nonzero even at the most positive potentials investigated; part of this curvature could still be caused by a potential dependent change in one or more of the other quantities mentioned in the text (including pK_a).

(43) Creager and Clarke studied mixed monolayers consisting of an ω-carboxylic acid alkanethiol and a normal-alkanethiol diluent.[3] The pK_a reported in the text is an average of those obtained for 11-mercaptoundecanoic acid in nonanethiol and decanethiol diluents.[3] The ionic strength given in the text is the ionic strength of the buffer solution used by Creager and Clarke (buffer capacity = 0.01 M) at pH = 6.4.

(44) Hu, K.; Bard, A. J. *Langmuir* **1997**, *13*, 5114.

(45) Goddard, E. D. *Adv. Colloid Interface Sci.* **1974**, *4*, 45.

(46) Fernandez, M. S.; Fromherz, P. *J. Phys. Chem.* **1977**, *81*, 1755.

(47) Mukerjee, P.; Banerjee, K. *J. Phys. Chem.* **1964**, *68*, 3567.

(48) Rossotti, F. J. C.; Rossotti, H. *The Determination of Stability Constants and Other Equilibrium Constants in Solution*; McGraw-Hill Book Company, Inc.: New York, 1961; p 21.

(49) Fawcett, W. R. *J. Electroanal. Chem.* **1994**, *378*, 117.

(50) Fawcett, W. R.; Fedurco, M.; Kováčová, Z. *Langmuir* **1994**, *10*, 2403.

(51) Barlow, C. A., Jr.; Macdonald, J. R. *J. Chem. Phys.* **1963**, *40*, 1535.

(52) Barlow, C. A., Jr.; Macdonald, J. R. *J. Chem. Phys.* **1965**, *43*, 2575.

(53) Macdonald, J. R.; Barlow, C. A., Jr. *J. Electrochem. Soc.* **1966**, *10*, 978.

(54) Liu, Y.-P.; Newton, M. D. *J. Phys. Chem.* **1994**, *98*, 7162.

(55) (a) Rebek, J., Jr.; Duff, R. J.; Gordon, W. E.; Parris, K. *J. Am. Chem. Soc.* **1986**, *108*, 6068. (b) Peterson, M. R.; Csizmadia, I. G. *J. Am. Chem. Soc.* **1979**, *101*, 1076. (c) Meyer, R.; Ha, T.-K.; Frei, H.; Günthard, Hs. H. *Chem. Phys.* **1975**, *9*, 383.

(56) Gandour, R. D. *Bioorg. Chem.* **1981**, *10*, 169.

(57) Creager, S. E.; Rowe, G. K. *J. Electroanal. Chem.* **1997**, *420*, 291.